ISSN 1028-334X, Doklady Earth Sciences, 2022, Vol. 507, Suppl. 3, pp. S349–S356. © Pleiades Publishing, Ltd., 2022.
Russian Text © The Author(s), 2023, published in Doklady Rossiiskoi Akademii Nauk. Nauki o Zemle, 2023, Vol. 508, No. 2, pp. 155–163.

GEOLOGY

Accretion of the Oceanic Crust in the Mid-Atlantic Ridge (48°–51.5° N) during "Dry" Spreading

A. A. Peyve[a],*, S. Yu. Sokolov[a], A. N. Ivanenko[b], A. A. Razumovskiy[a], I. S. Patina[a], V. A. Bogolubskiy[a], I. A. Veklich[b], A. P. Denisova[a], V. N. Dobrolyubov[a], S. A. Dokashenko[a], E. S. Ivanova[a], S. A. Lapina[a], I. A. Naumov[a], N. S. Nikitin[c], and Z. F. Urazmuratova[d]

Submitted by Academician K.E. Degtyarev October 4, 2022

Received October 4, 2022; revised October 13, 2022; accepted November 18, 2022

Abstract—This paper is based on geological and geophysical data obtained during the 53th expedition of the R/V *Akademik Nikolaj Strakhov*. We analyze the structure of the Mid-Atlantic Ridge segment, 400 km long, in the North Atlantic (between 48° N and 51.5° N). According to our studies, this segment is characterized by specific structures formed during the formation of the oceanic crust with a reduced supply of basaltic melts. This factor leads to tectonic outcropping of deep and mantle rocks of the lower crust during the continuous extension in the rift valley. These processes, called "dry" spreading, were previously unknown in the North Atlantic.

Keywords: North Atlantic, "dry" spreading, oceanic core complexes, Mid-Atlantic Ridge, non-transform displacements

DOI: 10.1134/S1028334X22601444

In 2022 the Geological Institute of Russian Academy of Sciences, organized and conducted the 53rd cruise of the R/V *Akademik Nikolai Strakhov* in the North Atlantic. The main purpose of the expedition was to carry out integrated geological and geophysical studies to obtain new data on tectonic, magmatic, and hydrothermal–metamorphic processes in the central part of the Mid-Atlantic Ridge (MAR) between 48° N and 51.5° N, south of the Charlie Gibbs transform fault on the Faraday study area, named after the mountain located in the central part of the area studied (Fig. 1).

During the cruise, data were collected simultaneously with the SeaBat 7150 multibeam echo sounder and the EdgeTech 3300 profiler. Anomalous magnetic field (AMF) data were recorded with the use of the SeaPOS2 magnetometer in the modification of a gradiometer. Seafloor sampling was performed by dredging. This work continued earlier studies of the MAR structures between the Byte and Charlie Gibbs transform faults [1–3].

Until now, nothing has been known about the structure and composition of the MAR crust to the south of 51.5° N, except for data on the compositions of basaltic glasses collected directly in the axial part of the rift valley of this segment [4]. We made a detailed bathymetric map on a scale of 1 : 100000 and a map of the anomalous magnetic field of the area between 48° N and 51.5° N, 80–90 km wide and about 400 km long on the basis of the data from the 53rd cruise. We also collected comprehensive rock material (28 successful seafloor dredgings) for further study (Table 1).

The analysis of the seafloor morphology has shown that the Faraday study area has a very complex structure. It changes in both the longitudinal and the latitudinal directions and may be conditionally divided into three segments. The Northern segment is located from 51.5° N to 50.2° N, the Central segment lies between 50.2° N and 49.7° N, and the Southern segment extends from 49.7° N to 48° N (Fig. 2).

The Northern segment in its northernmost part is a submeridional rift valley, 3900–3400 m deep and 6–7 km wide, framed by narrow, extended volcanic ridges to the east and west. South of 51.2° N, the morphology of the MAR is different. The rift valley gradually changes its strike from 5° to 312° and breaks up into a system of echelon-like rift valleys 10–15 km

[a] *Geological Institute, Russian Academy of Sciences, Moscow, 119017 Russia*
[b] *Institute of Oceanology, Russian Academy of Sciences, Moscow, 117997 Russia*
[c] *Moscow State University, Moscow, 119991 Russia*
[d] *Baltic Federal University, Kaliningrad, 236016 Russia*
**e-mail: apeyve@yandex.ru*

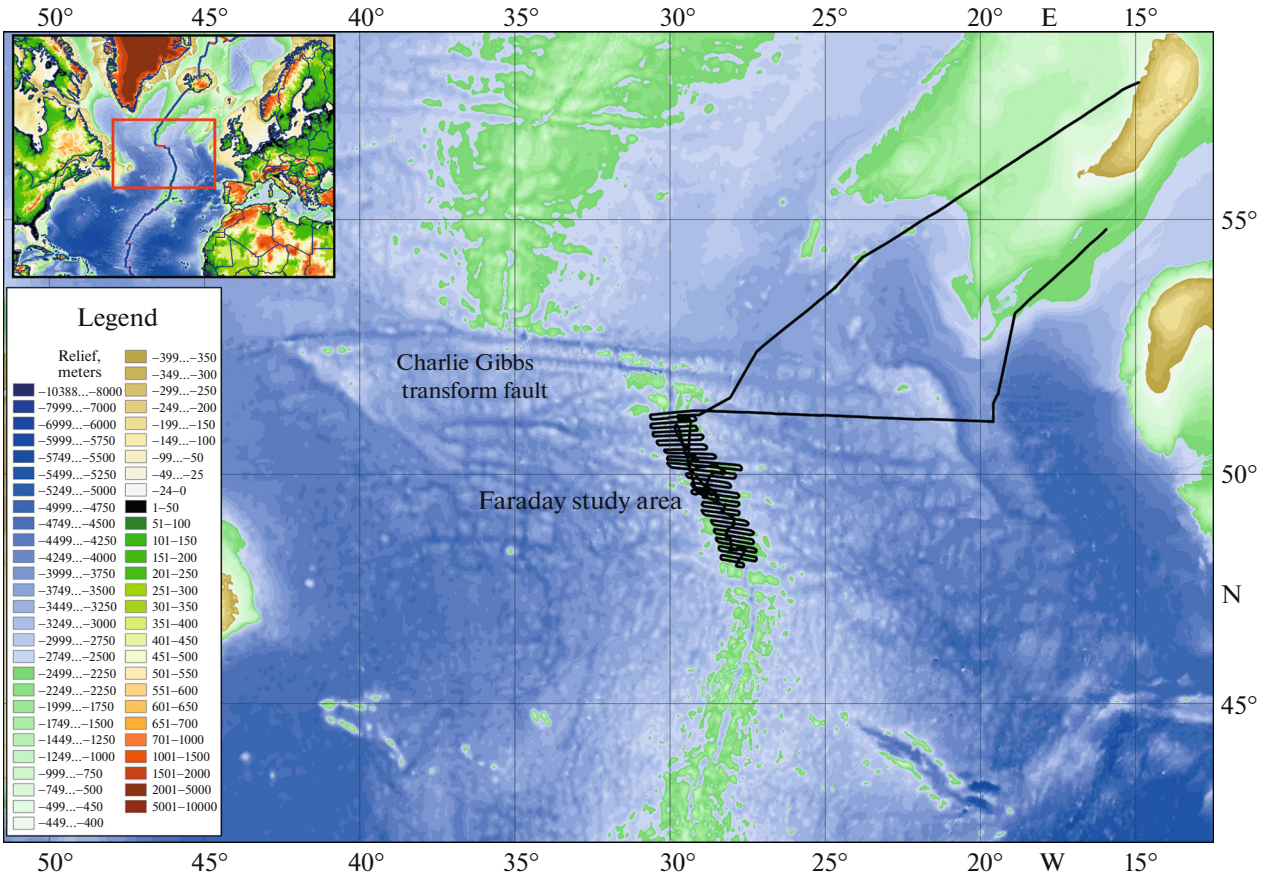

Fig. 1. The location scheme of the work area and the route of the 53rd cruise of the R/V *Akademik Nikolai Strakhov*.

long. The valleys, extended in the meridional direction, are separated by short and narrow neovolcanic rises, some of which are located on small isometric volcanic plateaus. The heights of the rises are 500–600 m. In terms of morphology, the main part of the Northern segment of the rift valley is formed under the kinematic conditions of oblique spreading. The results of dredging showed that the structures in the rift valley are formed by young lava flows with freshly quenched glass.

To the east and west of the rift valley, southward of 51.2° N, the ridge relief is dramatically changed to chaotic landforms, represented by both oval and isometric rises, in some places connected by branching low (200–400 m) ridges, which, in general, create cellular relief. It is difficult to speak of a single strike of these structures. Nevertheless, the separate submeridional linear structures are visible, as are the structures with a strike corresponding to the rift valley strike, which varies from 5° to 312° in the southerly direction.

Two large oval dome-like rises (Fig. 2) on the eastern flank of the MAR at 51.1° N latitude with apices less than 1 km deep were dredged. It was revealed that the rises are composed of tectonized rocks from the lower crust and upper mantle (stations S5331 and S5332) along with basalts. The morphology of the rises corresponds to the so-called oceanic core complexes (OCC), which are formed in the areas with a reduced input of melts during the tectonic outcropping of deep rocks to the surface along the low-angle normal faults [5, 6].

We do not have comprehensive information on the composition of rocks on the MAR flanks of the northern segment. However, in considering the chaotic morphology and almost complete absence of a system of elongated ridges, we can assume that deeper rocks also play a significant role in the structure of this region. Therefore, the bended segment of the rift valley between the meridional segments can be considered as a large nontransform displacement on the basis of morphology (at least in the southern part). Scattered accommodation of shear stresses occurs within this segment as in a system of oceanic plates.

The transition to the Central segment is abrupt. The strike of the rift valley becomes 355°, which corresponds to the orthogonal (normal) spreading. The short meridional section of the rift valley, 26 km long and 5–8 km wide in the axial part, rises to depths of 3400 m (from 4100 m). To the west and east, this zone of the rift valley is replaced by a series of closely

Table 1. Successful dredging stations of the 53rd cruise of R/V *Akademik Nikolai Strakhov* at the Faraday study area

Drag no.	N	W	Depth interval (m)	Percentage and weight (given without sediments and material of ice rafting)	Weight (kg)
S5303	50°31.7′	–29°29.3′	3880–3800	Basalts 100%	300
S5304	50°44.8′	–29°41.4′	3680–3500	Basalts 100%	70
S5305	51°00.1′	–29°48.4′	3820–3110	Basalts 98%, dolerites 2%	200
S5306	49°35.4′	–28°39.5′	2300–1800	Basalts 25%, dolerites 25%, gabbro 50%	30
S5307	49°34.5′	–28°29.8′	3670–2440	Basalts 95%, dolerites 1%, gabbro 4%	25
S5308	49°42.3′	–28°50.6′	3060–2770	Dolerites 20%, gabbro 80%	0.5
S5309	49°56.4′	–28°44.8′	2900–2700	Basalts 100%	80
S5310	50°02.4′	–28°37.2′	2550–2280	Gabbro 1%, ultramafic rocks 99%	50
S5311	50°01.2′	–28°36.8′	3000–2550	Basalts 15%, dolerites 5%, gabbro 10%, ultramafic rocks 70%	60
S5312	50°02.5′	–28°14.1′	3060–3060	Gabbro 100%	0.05
S5313	50°03.6′	–28°15.4′	2600–2400	Dolerites 5%, gabbro 10%, ultramafic rocks 85%	150
S5314	50°11.8′	–28°29.6′	2270–2150	Basalts 3%, gabbro 30%, ultramafic rocks 67%	60
S5316	50°09.4′	–29°07.0′	2900–2100	Basalts 1%, dolerites 2%, gabbro 82%, ultramafic rocks 15%	200
S5317	50°12.3′	–29°23.9′	2300–2000	Basalts 90%, gabbro 5%, ultramafic rocks 5%	1
S5318	48°13.1′	–27°43.6′	3400–2280	Basalts 100%	50
S5319	48°23.9′	–27°34.4′	1870–1750	Basalts 97%, dolerites 3%	40
S5320	48°27.5′	–27°48.7′	1900–1800	Basalts 90%, dolerites 10%	20
S5321	48°24.1′	–27°50.6′	2200–2050	Basalts 100%	7
S5322	48°24.8′	–28°01.4′	2150–1600	Basalts 100%	20
S5323	48°41.0′	–28°07.4′	2500–2300	Gabbro 100%	5
S5324	48°56.4′	–27°57.0′	2270–2000	Basalts 10%, ultramafic rocks 90%, limestones <1%	80
S5326	49°14.6′	–28°17.2′	2600–1800	Basalts 95%, dolerites 5%	350
S5327	49°21.7′	–28°12.7′	2480–2040	Ultramafic rocks 100%	50
S5328	49°38.8′	–29°06.3′	2100–1880	Basalts 100%	0.3
S5329	50°09.7′	–29°23.8′	2400–1650	Basalts 80%, dolerites 20%	5
S5330	50°12.6′	–29°25.8′	2280–1930	Basalts 95%, dolerites 5%	25
S5331	51°07.2′	–29°36.6′	2230–1900	Basalts 25%, gabbro 75%	30
S5332	51°07.7′	–29°43.1′	2200–1570	Basalts 60%, dolerites 5%, ultramafic rocks 35%, limestones <1%	100

located large isometric and submeridional rises. This series rises to depths of 1300 m and forms linear ridges 15–20 km wide, extending along the 286° (West) and 88° (East) azimuth. These ridges can be traced over distances of 200 km and 135 km, which suggests that the geodynamic system, which caused the formation of these structures, has existed for a long time. If the strike of the Eastern ridge generally corresponds to the direction of spreading (the divergence is only about 3°), the divergence for the Western ridge is 21°. This divergence can be explained by the fact that, over a long time, the American Plate has been displaced relative to the zone of generation of the new crust in the spreading area in the northwestern direction. This also follows from the data on modern vectors of plate motion measured on the continents and on rare stations on islands [7]. The motion vector of the American Plate has a smaller angle to the strike of the spreading axis than the vector of the Eurasian Plate. Due to this fact, in conjunction with the latitudinal spreading, the American Plate moves to the northwest relative to the Eurasian Plate. According to the dredging data, the Eastern ridge is composed generally of serpentinized and tectonized ultramafic rocks at 70%. Gabbro accounts for about 25%; basalts and dolerites, 5%. Within the Western ridge, basalts and dolerites predominate at 75%. Here, gabbro accounts for about 20% and ultramafic rocks, 5%.

Further to the south, the rift valley dramatically changes its strike to 312°, i.e., it is oriented in the same way as the southern part of the rift valley of the Northern segment. Its width increases to 14 km, and it is divided into several troughs stretched in the meridional direction, up to 4250 m deep, separated by narrow, short (3–5 km) ridge-like rises 200–300 m high.

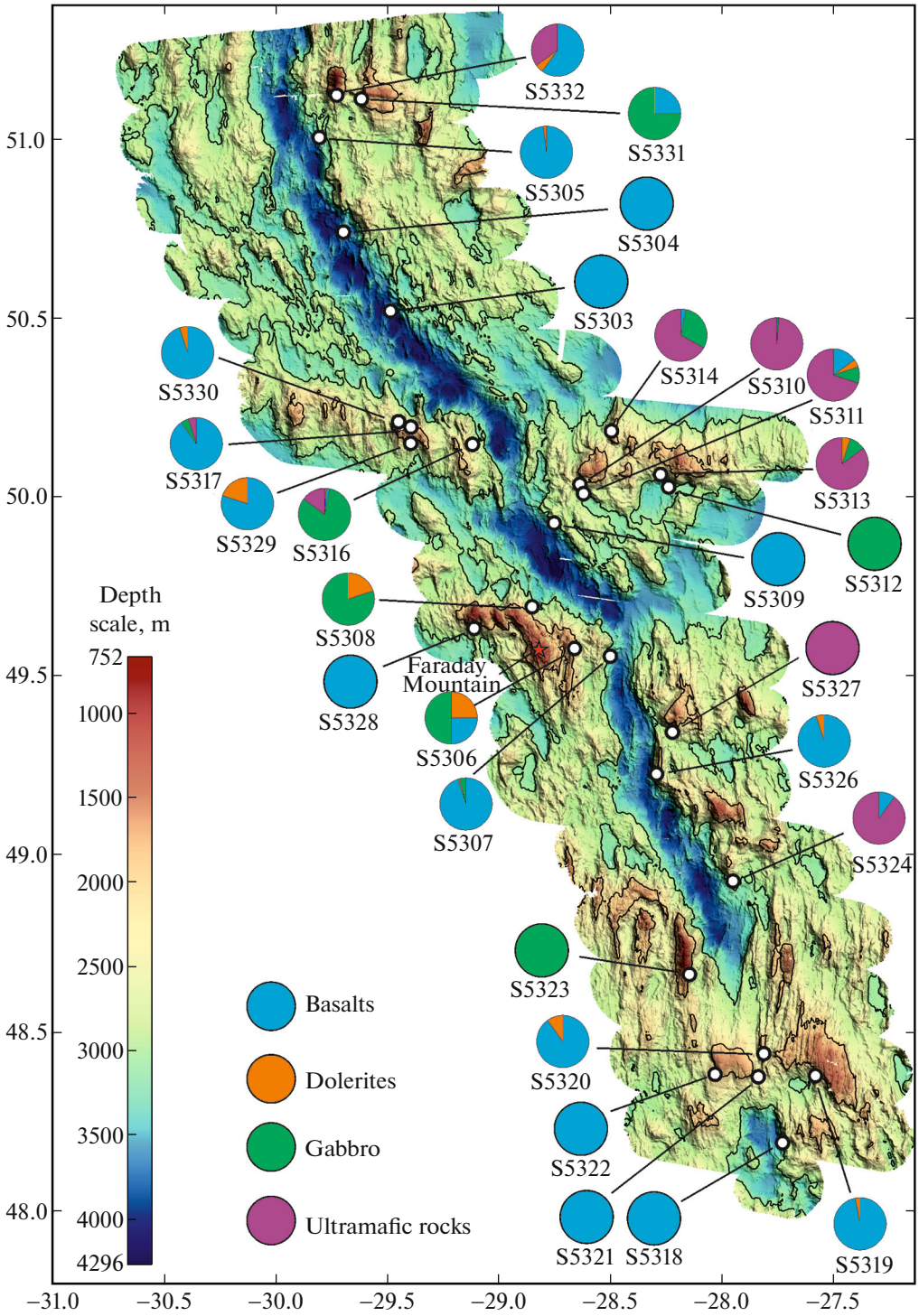

Fig. 2. Scheme of relief of the Faraday stydy area. The ratios of the dredged-up rocks are shown in the form of sectors. The isobaths are shown for the depths of 2000 and 3000 m.

On both sides of the rift valley, there are several parallel ridges of 300–400 m in height, located on the leveled (partially filled with sedimentary material) stepped plateau with depths of 3500–3400 m. The strike of the ridges corresponds to the strike of the rift valley axis.

South of 49.7° N (South segment), the rift valley again becomes submeridional, and its depth and width decrease to 3400–3800 m and 4–7 km, respectively. A system of similarly striking linear ridges, which, in some places, discordantly adjoins with isometric, sometimes, oval rises, is traced eastward of the rift val-

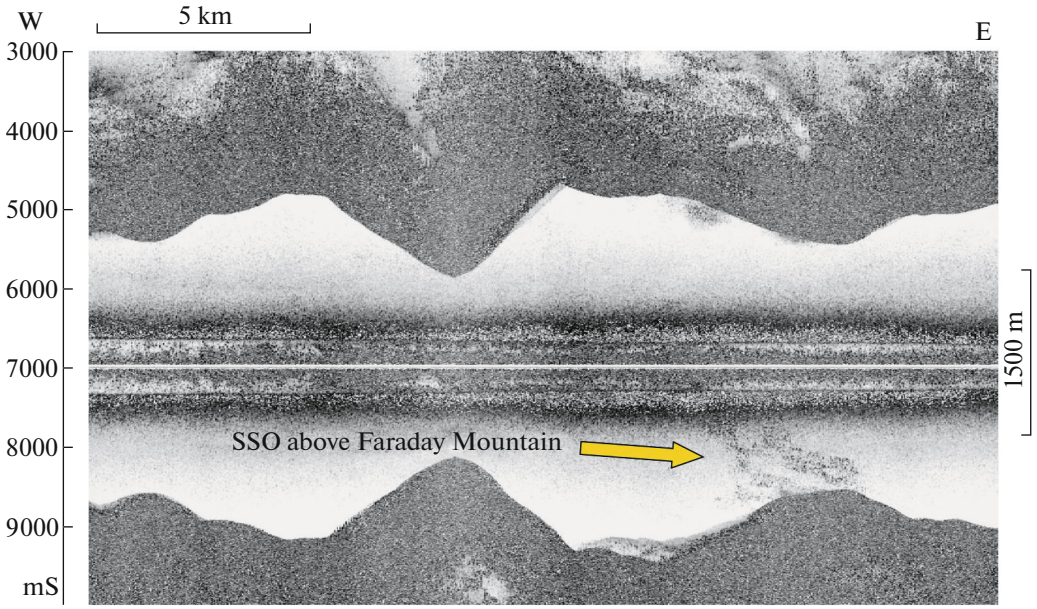

Fig. 3. Fragment of the sonar data with SDO over Faraday Mountain. The mountain position is shown in Fig. 2.

ley. The rise tops occur at shallow depths of 1500–1100 m rising above the oceanic floor at a height of 1500–1300 m. The chain of these structures can be traced eastward for at least 110 km along the 94°–95° azimuth. During the seafloor dredging of one of these rises (S5327), only serpentinized ultramafic rocks were found. The morphological features allow us to assume that similar structures are also composed of deep rocks.

To the west of the rift valley, there is a similar discordant system of rises. The system also combines the linear extended ridges typical for the volcanic relief within the rift valley, and the large dome-like rises generally characterized by a rounded or complex isometric shape. In this case, the minimum depth of one such rise (Faraday Mountain) is 752 m. According to the dredging data, the rises of the western flank of MAR at latitude 49.6° are mostly composed of gabbro (50–60%) and basalts and dolerites (50–40%). These structures in the form of a ridge can be traced westward for 60 km along the azimuth of 277°. To the west, there are separate large isometric rises, which do not form a single extended linear structure.

Analysis of the sonar data of a multibeam echo sounder in the Faraday Mountain area showed the presence of strong sound-scattering objects (SSOs) in the water column (Fig. 3).

The SSOs rise from the seafloor surface to the near-surface sound-scattering layer, which may be either hydrophysical or biogenic in origin. The deeper SSOs with seafloor roots in the MAR area are a rare phenomenon and may be caused by the ejection of hydrophysical contrasting solutions from a hydrothermal source. The hydrothermal origin and connection with potential ore-bearing capacity can be confirmed only by additional studies.

Further south, up to 48.7° N, the southern segment is a system of submeridional rift valleys, about 10–15 km long, consistently displaced eastward by 6–8 km. The entire rift valley bends smoothly, while the rift troughs and neovolcanic ridges within the rift valley retain a sublongitudinal orientation and form a system of echelon-like, second-order structures overlapping in some places. A complex combination of volcanic linear structures and variously oriented rises of various shapes and amplitudes, probably formed by tectonic processes, is observed.

The rift valley, as a morphological structure, is almost absent for 55 km between 48.2° N and 48.7° N. In its place, at a depth of 1660–1700 m, there is a large oval-shaped rise measuring 6–14 km at the top part. It transforms into a system of linear ridges and troughs to the west and east. There are also several isometric troughs, which may be associated with the pre-existing rift troughs. The dome-like rise is characterized by a flattened top surface. There are no rift ridges here, and, on the contrary, the relief has features similar to OCC structures. Only basalts (S5319–S5321) have been dredged from the eastern part of this rise. However, meridional rift ridges are well developed on this flank. Therefore, at this stage of investigations, the entire structure blocking the rift valley at 48.3°–48.6° N and 28.1°–27.3° W may be considered as a volcanic rise and its formation may be associated with a local thermal anomaly. Due to the fact that this rise has no visible continuation in the more ancient parts of the oceanic plate (it is localized within the rift valley and the first–second ridges of the rift mountains), this is a

young structure. However, its western part, where there is no rift-related relief, may involve deep rocks, which requires additional study. The freshest basalts were dredged on the western flank of the rise, suggesting that the spreading axis is currently located in the western part of the rift valley.

The rock material dredged at the Faraday study area is very diverse in composition, in the degree of secondary alterations, and in the tectonic transformations. The volcanics from the rift valley are represented by pillow lava fragments of generally micro- and fine-grained aphyric basalts with quenched glass. Plagiophyric varieties with large plagioclase phenocrysts are less common.

The basalt fragments from the sides of the rift valley have special features: smoothed edges and traces of the secondary alteration, and quenched glass is more palagonitized. This may indicate significant interruptions in volcanic activity even within the rift valley itself. Both the degree of rounding and the degree of the secondary low-temperature alteration increase in basaltic fragments (S5332, S5331, S5330, S5317, S5329, S5328, S5306) as they move away from the rift valley into the limits of the rift ridges.

Dolerites were dredged together with fragments of pillow basalts and can be interpreted either as well-crystallized parts of relatively thick flows or as dikes of feeder channels. Sometimes dolerites were dredged together only with gabbro and ultramafic rocks. In this case, we can assume that we are dealing with rocks of the feeder channels, which are complementary to modern lavas, or with the central parts of relatively powerful lava flows. At the same time, we cannot exclude the possibility that we see fragments of a dyke complex here.

The rocks of the layered complex of the lower crust (united by the term gabbro) are mainly large- and giant-crystalline gabbro, olivine gabbro, and troctoliths. The rocks are massive or taxitic, often irregularly grained with pegmatoid segregations. Some have a banded flaser structure corresponding to high-temperature solid-plastic deformations. Some samples also contain orthopyroxene. An overwhelming number of gabbro are transformed by low-temperature metamorphic processes. Pyroxenes are amphibolized and chloritized, plagioclase is replaced by prehnite and clay minerals. The rocks of this association were dredged almost everywhere (except for the rift valley) within both dome-like rises and extended linear ridges. Often the rocks are intensely tectonized: fractured with sliding mirrors, affected by cleavage and/or cataclasized. In some cases, this phenomenon has the features of near-surface disintegration, with the filling of cracks with an organogenic–sedimentary matrix. At the same time, there are rocks with serpentinite–clasts and gabbro–crystalloclasts, which bear the features of tectonic cataclasis, and some of them may be partially recrystallized during these processes.

On the rise with the center at 51.1° N and 29.5° W (station S5331), all fragments of gabbro contain ore mineralization (station S5331) and all gabbro debris contains ore mineralization. The total amount of the ore component may be up to 10% of the rock volume.

Ultramafic rocks (mantle peridotites) are represented, to a high degree, by strongly (often 100%) serpentinized harzburgites and, sometimes, dunites. The rocks are represented both by massive varieties with initial porphyroclastic and granoblastic structures, formed as a result of several stages of viscous-plastic deformation, and completely schistose varieties transformed into chrysotile-asbestos schists. Intense limonitization and hematization are noted for some tectonized varieties. In some samples, there are cross veins of gabbro. The dredging showed that ultramafic rocks mostly are dredged within the dome-like rises east of the rift valley.

The anomalies identified by the results of magnetic survey (Fig. 4) are symmetrical relative to a central anomaly and have a clear correlation from profile to profile, creating a typical sequence of linear magnetic anomalies of spreading origin [8].

The central anomaly corresponds to the Brunhes geomagnetic epoch (0–0.78 Ma). The anomaly extends through the entire study area, has a sinuous strike, changing the azimuth from strictly longitudinal to 315°–320°. Its position almost repeats the bends of the rift valley. This is obvious in combining the magnetic and bathymetric data. Rift anomaly 2 (negative, 0.78–4.19 Ma), which is traced on both sides of the rift, is conformable to the central anomaly and includes 2A (positive, 2.58–3.6 Ma), which have a typical shape and are easy enough to identify.

Identification of the anomalies made it possible to calculate the spreading velocities. In general, the spreading velocity within the Faraday study area remains stable and lies within 10–12 mm/yr. The latter is especially typical of the western flank of MAR, where the velocity decreases gradually from 12 mm/yr in the north to 9.7 mm/yr in the south. This indicates a relatively stable tectonic setting to the west of the MAR axis. A more complicated picture is observed to the east of the MAR axis. Here, the average opening rate and variability are slightly higher (12–13 mm/year) than in the west.

In the area of profiles 11–15 (50° N–50.3° N, 29° W) in the rift valley, the intensity of the central anomaly becomes weak; it expands and then splits into two branches. It is possible that here we observe an attempt to "jump" the spreading axis eastward by about 20 km, which, however, did not lead to the formation of a transform fault. This probably explains the reduced spreading velocities in profiles 10 and 12. The expansion of the rift zone and, correspondingly, 1st anomaly "ate" the part of the crust that had an age and reverse magnetization corresponding to the beginning of the 2nd anomaly. A similar situation is observed in the

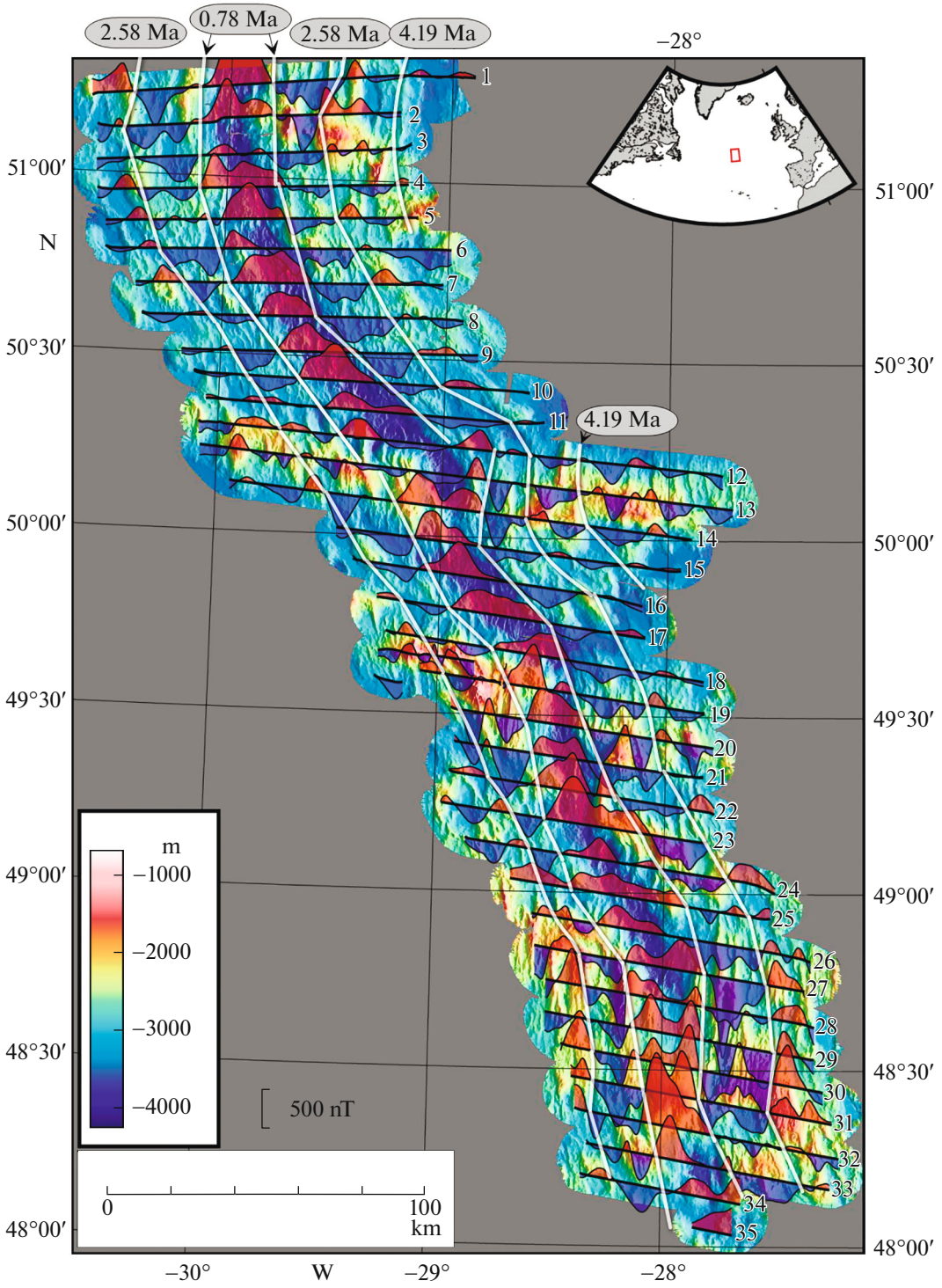

Fig. 4. The map of the plots of the anomalous magnetic field, superimposed on the map of the seafloor relief at the Faraday study area. Numbers indicate the survey profiles, white lines are isochrons, and numbers in ovals are the age of the lithosphere according to the distinguished linear magnetic anomalies.

southern part of the study area, in the area of profiles 28–32 (48.3°–48.7° N, 28° W).

Therefore, the segment of MAR between 48° and 51.5° N has a very complex structure. The areas where the rift valley has a longitudinal strike alternate with the areas where the rift valley strike changes to the northwesterly direction. A bend of the rift valley occurs without breaking its continuity, which is char-

acteristic of the so-called nontransform displacements. In fact, all sections of the northwest-striking rift valley can be considered as extended areas of the nontransform displacements, where the oceanic crust is accreted during oblique spreading. No signs of large strike–slip faults, which are typical of transform faults, are observed. The relative displacement of zones of the oceanic lithosphere is realized in the form of elongated areas, which are entirely the accommodation zones of stresses arising during the motion of the lithospheric plates.

The main result of the research is that for the first time in the North Atlantic a MAR segment of about 400 km long (between 48° and 51.5° N) has been studied. This zone is characterized by the formation of the oceanic crust under the conditions of basaltic melt deficiency. During continuous stretching in the rift valley, this setting leads to tectonic outcropping of the deep lower crust and mantle rocks to the seafloor surface. Such processes, called "dry" spreading, have been described in the MAR zones of the Central Atlantic with low velocities of new crust formation [9–12], but they had not been known north of 34° N.

FUNDING

This work was conducted according to State Assignments (FMMG-2022-0003, FMUN-2019-0076, and FMWE-2021-0005).

CONFLICT OF INTEREST

The authors declare that they have no conflicts of interest.

REFERENCES

1. S. G. Skolotnev, A. A. Peyve, A. Sanfilippo, A. N. Ivanenko, M. Ligi, I. A. Veklich, L. Petracchini, V. Basch, D. A. Kuleshov, C. Ferrando, V. N. Dobrolyubov, C. Sani, N. A. Shkittin, M. Bickert, S. A. Dokashenko, F. Muccini, E. S. Yakovenko, K. Palmiotto, and M. Cuffaro, Dokl. Earth Sci. **504** (1), 233–240 (2022).
2. S. G. Skolotnev, A. Sanfilippo, A. A. Peyve, Y. Nestola, S. Yu. Sokolov, L. Petracchini, K. O. Dobrolyubova, V. Basch, A. N. Pertsev, C. Ferrando, A. N. Ivanenko, C. Sani, A. A. Razumovskii, F. Muccini, A. S. Bich, C. Palmiotto, Yu. V. Brusilovskii, E. Bonatti, K. N. Sholukhov, M. Cuffaro, I. A. Veklich, M. Ligi, and V. N. Dobrolyubov, Dokl. Earth Sci. **497** (1), 191–195 (2021).
3. S. G. Skolotnev, A. Sanfilippo, A. A. Peyve, Y. Nestola, S. Yu. Sokolov, L. Petracchini, K. O. Dobrolyubova, V. Basch, A. N. Pertsev, C. Ferrando, A. N. Ivanenko, C. Sani, A. A. Razumovskiy, F. Muccini, A. S. Bich, C. Palmiotto, Yu. V. Brusilovsky, E. Bonatti, K. N. Sholukhov, M. Cuffaro, I. A. Veklich, V. N. Dobrolyubov, and M. Ligi, Ofioliti **46** (1), 83–101 (2021).
4. J.-G. Schilling, M. Zajac, R. Evans, T. Johnston, W. White, J. D. Devine, and R. Kingsley, Am. J. Sci. **283**, 510–586 (1983).
5. H. J. B. Dick, M. A. Tivey, and B. E. Tucholke, Geochem., Geophys., Geosyst. **9** (5), 1–44 (2008).
6. C. J. MacLeod, R. C. Searle, J. F. Casey, C. Mallows, M. Unsworth, K. Achenbach, and M. Harris, Earth Planet. Sci. Lett. **287**, 333–344 (2009).
7. W. Shimin, Yu. Hongzheng, Z. Qiong, and Z. Yonghong, Earth Planet. Sci. Lett. **490**, 88–99 (2018).
8. S. Merkouriev and C. DeMets, Geophys. J. Int. **198**, 366–384 (2014).
9. E. Gracia, J. Charlou, J. Radford-Knoery, and L. Parson, Earth Planet. Sci. Lett. **177**, 89–103 (2000).
10. A. A. Peyve, Geotectonics **38** (6), 405–418 (2004).
11. A. A. Peyve, G. N. Savel'eva, S. G. Skolotnev, and V. A. Simonov, Geotectonics **37** (2), 75–95 (2003).
12. M. Cannat, D. Sauter, V. Mendel, E. Ruellan, K. Okino, J. Escartin, V. Combier, and M. Baala, Geology **34** (7), 605–608 (2006).

Translated by V. Krutikova